INFORMATICA, 2013, Vol. 24, No. 4, 505–521

Computational Modeling of Bienzyme Biosensor with Different Initial and Boundary Conditions

Vytautas AŠERIS[1*], Romas BARONAS[1], Juozas KULYS[2]
[1]*Faculty of Mathematics and Informatics, Vilnius University, Naugarduko 24, LT-03225 Vilnius, Lithuania*
[2]*Institute of Biochemistry, Vilnius University, Mokslininkų 12, LT-08662 Vilnius, Lithuania*
e-mail: vytautas.aseris@mif.vu.lt, romas.baronas@mif.vu.lt, juozas.kulys@bchi.vu.lt

Received: September 2012; accepted: February 2013

Abstract. Two mathematical models of an amperometric bienzyme biosensor are analysed digitally. The models hold different boundary conditions describing the singularity of the electrode (transducer). The influence of the initial and boundary conditions on the biosensors action at different sets of parameters is analysed.

The digital simulation at the transient and steady-state conditions was carried out by using finite difference technique. The comparison of the simulation results revealed that some of the calculated parameters, i.e. response and sensitivity is the same, while the others, i.e. half-time of the steady-state is significantly different for distinct models.

Key words: modelling; biosensor; catalase; peroxidase; diffusion.

1. Introduction

Biosensors are analytical devices used for the detection and recognition of the chemical substances in the solutions to be analysed (Scheller *et al*., 1997; Sadana and Sadana, 2010). Biosensors containing biological catalysts are analysed in this paper. Such biosensors are widely applied in medicine, ecology and environmental monitoring (Cooper and Cass, 2003).

The computational modelling is applied in various scientific areas, i.e. the modelling of blood glucose dynamics (Basov and Švitra, 2000), anisotropic media (Kleiza *et al.*, 2007), moisture diffusion in wood (Baronas *et al*., 2002) and others. For almost half a century the mathematical modelling was also used to investigate the behaviour of the biosensors (Mell and Malloy, 1975; Schulmeister, 1990). The computational modelling is widely used instead of expensive physical experiments aiming at understanding the kinetic peculiarities of the biosensors (Baronas *et al*., 2010; Dabulytė-Bagdonavičienė *et al*., 2011).

The computational modelling of biosensors is complicated and time-consuming task (Ahuja, 2010; Britz, 2005). In most cases the finite difference technique is employed

*Corresponding author

and the software implementing the computational model is created (Baronas *et al*., 2010; Bieniasz and Britz, 2004). Various finite difference schemes have been analysed and compared to model the behaviour of the classical Michaelis–Menten biosensor (Britz *et al*., 2009). The improvement of the finite difference schemes to solve similar problems was presented by Bieniasz in the 15 part series from Bieniasz (1993) to Bieniasz (2004). However, the most important part of the biosensor computational modelling is creating the adequate and valid mathematical model for a concrete system of biochemical reaction-diffusion equations, describing the kinetic action. Such mathematical model of the biosensor using parallel substrate conversion is presented in this paper.

Various biosensors utilizing multi step and parallel conversion of substrates have been developed (Kulys *et al*., 1986; Akkaya *et al.*, 2009). A mixture of substrates, participating in independent reactions described by Michaelis–Menten kinetics was analysed in Žilinskas and Baronas (2011). Optical biosensors were computationally investigated in Rickus (2005). The use of catalase and peroxidase as the enzymes enabling parallel substrates conversion was recently investigated in our previous work (Ašeris *et al*., 2012). A specific boundary condition was used to describe the electrode working as a transducer in Ašeris *et al*. (2012). Different boundary conditions are usually used in modelling biosensors based on different electrodes (Scheller *et al*., 1997; Baronas *et al*., 2010; Schulmeister, 1990). In this work we investigate the influence of the singularity of the boundary conditions on the biosensor action. An additional more comprehensive analysis of the diffusion module was carried out after noticing some patterns in our previous work.

The biochemical reaction of catalase-peroxidase is described by the following kinetic scheme:

$$S_1 \xrightarrow{E_1} \frac{1}{2} P_1, \qquad S_1 + S_2 \xrightarrow{E_2} P_2, \tag{1}$$

where S_1 and S_2 denote first and second substrates, respectively, P_1 and P_2 are the reaction products, E_1 stands for catalase and E_2 – for peroxidase. A wide variety of electrodes are used in practice for the determination of the product concentrations (Morf *et al*., 2011; Baronas *et al*., 2008). The molecular oxygen (P_1) can be effectively detected by applying a sensitive to oxygen electrode. A Clark-type electrode (CE) measures oxygen on a catalytic platinum surface, while the oxygen itself is not consumed to generate current (Rodriguez-López *et al*., 1992). Alternatively, the electrode can be so polarized that the concentration of the reaction product at the electrode surface is being permanently reduced to zero. An electrode of this type is called Non-Clark-type electrode (NCE).

The operation of the biosensors to be analysed is two-phased: in the first phase, only the first substrate (hydrogen peroxide) is present in the solution. The response of the biosensor reaches the steady-state at the end of the first phase. At the beginning of the second phase the second substrate is poured into the solution. At the end of the second phase the response of the biosensor is different in a value from the one in the first phase. The relative difference between the responses at the steady-state in both phases is measured as the final response of the biosensor to determine the concentration of the second substrate.

Different electrodes might be used to detect the concentration of the molecular oxygen at the electrode surface. The goal of this investigation was to compare how different electrodes affect the biosensors behaviour at the different conditions of the biosensors operation. Two computational models with different boundary conditions were developed and analysed at various sets of parameters. Normalized concentration profiles were investigated at the steady-state for both biosensors. The dependency of the half time of the steady-state on the Biot number and on the substrate concentration was also investigated.

2. Mathematical Modelling

Both mathematical models involve three regions in the one-dimensional space: the enzymatic and the diffusion layers and a convective region. The biosensor operation is described by non-linear reaction-diffusion equations. Biosensors utilizing a Non-Clark-type electrode (NCE) and a Clark-type electrode (CE) for the oxygen detection are modelled in this section.

2.1. *Governing Equations*

Coupling the enzymes catalyzed reactions 1 in the enzyme layer with the mass transport by diffusion, described by Fick's law, leads to the following system of the reaction diffusion equations ($0 < x < d$, $t > 0$):

$$\frac{\partial s_{1,e}}{\partial t} = D_{s_{1,e}} \frac{\partial^2 s_{1,e}}{\partial x^2} - r_1 - r_2, \qquad \frac{\partial s_{2,e}}{\partial t} = D_{s_{2,e}} \frac{\partial^2 s_{2,e}}{\partial x^2} - r_2, \tag{2}$$

$$\frac{\partial p_{1,e}}{\partial t} = D_{p_{1,e}} \frac{\partial^2 p_{1,e}}{\partial x^2} + \frac{1}{2} r_1, \qquad \frac{\partial p_{2,e}}{\partial t} = D_{p_{2,e}} \frac{\partial^2 p_{2,e}}{\partial x^2} + r_2, \tag{3}$$

$$r_1 = k_1 e_1 s_{1,e}, \qquad r_2 = \frac{k_{21} k_{22} e_2 s_{1,e} s_{2,e}}{k_{21} s_{1,e} + k_{22} s_{2,e}}, \tag{4}$$

where x and t stand for space and time, respectively, $s_{1,e}(x,t)$, $s_{2,e}(x,t)$, $p_{1,e}(x,t)$ and $p_{2,e}(x,t)$ are the molar concentrations of the substrates S_1, S_2 and the products P_1, P_2 in the enzyme layer of the thickness d, respectively, and $D_{s_{1,e}}$, $D_{s_{2,e}}$, $D_{p_{1,e}}$ and $D_{p_{2,e}}$ are the constant diffusion coefficients.

Outside the enzyme layer ($d < x < \delta$, $t > 0$) only the mass transport of all the species by the diffusion takes place,

$$\frac{\partial c_d}{\partial t} = D_{c_d} \frac{\partial^2 c_d}{\partial x^2}, \quad c = s_1, s_2, p_1, p_2, \tag{5}$$

where $c_d(x,t)$ is the molar concentration of the corresponding substrate or product in the diffusion layer of the thickness δ, and D_{c_d} is the diffusion coefficient.

2.2. *Initial Conditions*

At the beginning of the biosensor operation ($t = 0$) no substances are present in the buffer solution, the enzymatic and the diffusion layers,

$$\begin{aligned} &c(x, 0) = 0, \quad 0 < x < d + \delta, \\ &c = s_{1,e}, s_{2,e}, p_{1,e}, p_{2,e}, s_{1,d}, s_{2,d}, p_{1,d}, p_{2,d}. \end{aligned} \tag{6}$$

Only the first substrate appears in the bulk at the beginning of the biosensor action ($t = 0$),

$$s_{1,d}(d + \delta, 0) = s_{10}, \tag{7}$$

where s_{10} is the concentration of the first substrate in the bulk. The second substrate is not present in the solution,

$$s_{2,d}(d + \delta, 0) = 0. \tag{8}$$

2.3. *Boundary Conditions*

Boundary conditions on the boundaries between the electrode and the enzymatic layer ($x = 0$), between the enzyme and diffusion layers ($x = d$) and between the diffusion layer and bulk solution ($x = d + \delta$) have to be defined. At the beginning ($t = 0$) of the biosensor operation some of the first substrate appears in the bulk.

In the case of the NCE electrode, due to the electrode polarization the reaction product is assumed to be constantly reduced to zero concentration at the electrode surface,

$$p_{1,e}(0, t) = 0. \tag{9}$$

The substrates and the second product are considered to be electrically inactive materials. This is defined by the following boundary condition ($t > 0$) at the electrode surface ($x = 0$):

$$D_{c_e} \left.\frac{\partial c_e}{\partial x}\right|_{x=0} = 0, \quad c = s_1, s_2, p_2. \tag{10}$$

The fluxes of the substrates and the products entering the enzymatic layer are considered to be equal to the outgoing ones. This is defined by the following matching conditions ($t > 0$):

$$D_{c_e} \left.\frac{\partial c_e}{\partial x}\right|_{x=d} = D_{c_d} \left.\frac{\partial c_d}{\partial x}\right|_{x=d}, \quad c = s_1, s_2, p_1, p_2, \tag{11}$$

$$c_e(d, t) = c_d(d, t), \quad c = s_1, s_2, p_1, p_2. \tag{12}$$

In the bulk the concentrations of both substrates are considered to be constant, while the concentration of the reaction products is constantly reduced to zero,

$$s_{1,d}(d+\delta,t) = s_{10}, \tag{13}$$

$$s_{2,d}(d+\delta,t) = \begin{cases} 0, & \text{if } t < T_1, \\ s_{20}, & \text{if } t \geqslant T_1, \end{cases} \tag{14}$$

$$p_d(d+\delta,t) = 0, \quad p = p_1, p_2, \tag{15}$$

where s_{20} is the concentration of the second substrate in the buffer solution, and T_1 is the time moment when the second substrate appears in the solution.

In the case of the Clark electrode (CE) the molecular oxygen is not consumed at the electrode surface, therefore the boundary condition (9) for the first product is replaced by the following one:

$$D_{p_{1,e}} \frac{\partial p_{1,e}}{\partial x}\bigg|_{x=0} = 0. \tag{16}$$

The time moment when the second substrate appears in the solution is marked by T_2 for the CE biosensor.

2.4. *Biosensor Response*

The anodic or cathodic current is assumed as the response of the amperometric biosensor (Bartlett *et al.*, 2008). The current density $i_1(t)$ can be obtained according to Fick's and Faraday's laws (Scheller *et al.*, 1997),

$$i_1(t) = n_e F D_{p_{1,e}} \frac{\partial p_{1,e}}{\partial x}\bigg|_{x=0}, \tag{17}$$

where F is Faraday's constant ($F = 96.486 \times 10^6\,\mathrm{CM}^{-1}\,\mathrm{m}^{-3}$), n_e is a number of electrons involved in the electrochemical reaction. We used $n_e = 2$ in all of the simulations. As one can see, the current density (17) is proportional to the flux of the reaction product at the electrode surface.

In the case of the Clark electrode the current density as the biosensor response is directly proportional to the product concentration at the electrode surface,

$$i_2(t) = k_s F p_{1,e}(0,t), \tag{18}$$

where k_s is the heterogenic constant calculated experimentally.

An action of the NCE-based biosensor was mathematically defined by (2)–(5), (6)–(8), (9)–(15) and (17). The mathematical model for the corresponding CE-based biosensor involves the following equations: (2)–(5), (6)–(8), (10)–(16) and (18).

3. Numerical Simulation

Because of the non-linear reaction term (4) in the governing equations (2), (4), the mathematical models of NCE and CE biosensors are solved analytically only for a specific set of parameter values (Schulmeister, 1990). A discrete grid was developed with a purpose to solve the problem numerically by using a finite difference technique. The grid was uniform in both directions (space and time) with 300 points for the enzymatic and the diffusion layers, each.

A number of methods exist to solve a finite difference scheme (Baronas *et al.*, 2010; Bartlett *et al.*, 2008; Samarskii, 2001) with various possible improvements (Bieniasz, 1993, 2004). A Crank-Nicolson finite difference scheme was built as a result of the difference approximation in order to solve the problem (Crank and Nicolson, 1947). The CN scheme was chosen as it has the appealing speed to stability ratio (Britz *et al.*, 2009). The digital simulators of both models were built in C++ programming language (Press *et al.*, 2007). The calculation times of both digital simulators were compared and the results showed that neither simulator runs more than twice faster.

3.1. *Biosensor Characteristics*

Both mathematically described systems approach the steady-state as $t \to \infty$,

$$i_{s,\alpha} = \lim_{t\to\infty} i_\alpha(t), \quad \alpha = 1, 2, \tag{19}$$

where $i_{s,1}$ and $i_{s,2}$ are the steady-state currents of the first (NCE) and the second (CE) biosensors, respectively.

A difference $i_{d,1}$ for NCE biosensor and $i_{d,2}$ for CE biosensor are measured in order to evaluate the concentration s_{20} of the second substrate S_2:

$$i_{d,\alpha} = i_{s_{10},\alpha} - i_{s_{20},\alpha}, \quad \alpha = 1, 2, \tag{20}$$

where $i_{s_{10},1}$ and $i_{s_{10},2}$ are the steady-state responses at zero concentration of the second substrate, $i_{s_{20},1}$ and $i_{s_{20},2}$ are the steady-state responses with a presence of the second substrate in the solution for NCE and CE biosensors, respectively.

We normalize the difference of the steady-state responses with the current $i_{s_{10},\alpha}$:

$$I_{r,\alpha} = \frac{i_{d,\alpha}}{i_{s_{10},\alpha}} = \frac{i_{s_{10},\alpha} - i_{s_{20},\alpha}}{i_{s_{10},\alpha}}, \quad \alpha = 1, 2, \tag{21}$$

where $I_{r,\alpha}$ is the relative steady-state biosensor current or the relative response.

The sensitivity is a characteristic indicating how properly the biosensor responds to the concentration changes of the substance to be analysed (Cooper and Cass, 2003; Sadana and Sadana, 2010). The sensitivity is defined as the gradient of the steady-state current with respect to the concentration of the substrate to be determined (Scheller *et al.*, 1997; Baronas *et al.*, 2010). In case of a sensitive biosensor, a relatively small increase in the

substrate concentration leads to a relatively large alteration in the biosensors response. In case of the catalase-peroxidase biosensor, we analyse the following dimensionless sensitivity (Ašeris *et al*., 2012),

$$B_{r,\alpha} = \frac{di_{d,\alpha}(s_{20})}{ds_{20}} \frac{s_{20}}{i_{d,\alpha}(s_{20})} = \frac{dI_{r,\alpha}(s_{20})}{ds_{20}} \frac{s_{20}}{i_{r,\alpha}(s_{20})}, \quad \alpha = 1, 2. \tag{22}$$

In digital simulation the time $t_{R\alpha}$ was used to describe the time when the response reaches the steady-state with accuracy of ϵ:

$$t_{R,\alpha} = \min_{t>T_\alpha} \left\{ t\colon \frac{t}{i_\alpha(t)} \left| \frac{di_\alpha(t)}{dt} \right| < \epsilon \right\}, \quad i_\alpha(t_{R,\alpha}) \approx i_{s,\alpha},\ \alpha = 1, 2, \tag{23}$$

where $t_{R,1}$ and $t_{R,2}$ are the assumed response times at the steady-state of the second operational phase of the biosensors. In calculations we used $\epsilon = 10^{-3}$. The decay rate ϵ highly influences the response time, when $\epsilon \to 0$, $t_R \to \infty$. The half time of the steady-state can be used to investigate the behaviour of the response time (Baronas *et al*., 2010). We used the half time of the steady-state of the second phase of the biosensor operation described as follows:

$$t_{h,\alpha} = \min_{t>T_\alpha} \left\{ t\colon\ i_\alpha(t) < i_\alpha(T_\alpha) - \frac{i_\alpha(T_\alpha) - i_\alpha(t_{R,\alpha})}{2} \right\} - T_\alpha, \quad \alpha = 1, 2, \tag{24}$$

where $t_{h,\alpha}$ is the time difference between the time when the reaction-diffusion process reaches the medium in the second operation phase and the time when the second substrate is poured into the bulk. It is the half of the time moment of occurrence of the half of the steady-state current in the second phase of the biosensor action.

In this paper the influence of both enzymes on the half time was investigated. The following dimensionless reaction rate ξ between the concentrations of the catalase and peroxidase and their kinetic reaction rates was introduced:

$$\xi = \frac{k_1 e_1}{k_{21} e_2}. \tag{25}$$

The thicknesses of the enzymatic and diffusion layers are the other important characteristics highly affecting the half time of the steady-state (Baronas *et al*., 2008, 2003). The Biot number includes the thicknesses of both layers,

$$Bi = \frac{d}{D_{s_{2,e}}} \times \frac{D_{s_{2,d}}}{\delta}. \tag{26}$$

As one can see the Biot number Bi expresses the ratio of the internal mass transfer resistance to the external one. The thickness δ of the diffusion layer, which is treated as the Nernst layer, is practically independent upon the enzyme membrane thickness d (Britz, 2005).

Another important characteristic of the biosensor is the diffusion module, known as the Damköhler number (Aris, 1975),

$$\sigma_1^2 = \frac{k_1 e_1 d_e^2}{D_{s_{1,e}}}, \qquad \sigma_2^2 = \frac{k_{21} e_2 d_e^2}{D_{s_{1,e}}}. \tag{27}$$

The diffusion modules σ_1 and σ_2 compare the rates of the enzymatic reactions $k_1 e_1$ and $k_{21} e_2$, respectively, with the diffusion rate $D_{s_{1,e}}/d_e^2$. The influence of the diffusion module on the other parameters of the biosensors are well established for Michaelis–Menten kinetics biosensors, biosensors based on a chemically modified electrode (Baronas *et al*., 2008), and others (Baronas *et al*., 2010). An impact of the diffusion module on the response and the sensitivity of the bienzyme biosensor is noted in our earlier publication (Ašeris *et al*., 2012). A more detailed analysis of the Damköhler number influence to the biosensor characteristics are carried out in this paper.

3.2. *Model Validation*

The first model was validated by using known analytical solutions for the steady-state at the specific set of parameter values (Schulmeister, 1990). The analytical solutions exist when second reaction term r_2 becomes linear when (a) $k_{21} s_{10} \ll k_{22} s_{20}$ and $k_1 e_1 \gg k_{21} e_2$; (b) $k_{21} s_{10} \gg k_{22} s_{20}$ and $k_1 e_1 s_{10} \gg k_{21} e_2 s_{20}$. Constant parameter values used in validation process are listed in Tables 1 and 2 (Bisswanger, 2008; Kulys *et al*., 2000; Andersen *et al*., 1991).

By choosing the values of the reaction rate constants k_{21} and k_{22} and concentrations of the substrates s_{10} and s_{20}, so that the analytical solution would be known, and keeping other parameters constant as listed in Table 1, and changing the remaining parameter values as displayed in Table 2, the relative difference between the analytical and computational steady-state current densities was less than 1% for the first mathematical model.

The mathematical model utilizing Clark-type electrode was validated by calculating the heterogenic constant k_s at a set of parameter values so that the response would be equal to the response of the first model at the steady-state. The responses at the steady-state of both biosensors were compared at different sets of parameter values by using the calculated heterogenic constant. The relative difference between the responses was identical for all the analysed cases.

Table 1
Constant values of the biosensor parameters.

Parameters	Notation	Value	Dimension
Diffusion coefficient	$D_{s_{1,e}}, D_{s_{2,e}}, D_{p_{1,e}}, D_{p_{2,e}}$	3×10^{-10}	$\mathrm{m^2\,s^{-1}}$
Diffusion coefficient	$D_{s_{1,d}}, D_{s_{2,d}}, D_{p_{1,d}}, D_{p_{2,d}}$	6×10^{-10}	$\mathrm{m^2\,s^{-1}}$
Reaction rate constant	k_1	10^7	$\mathrm{M^{-1}\,s^{-1}}$
Reaction rate constant	k_{21}	7.1×10^6	$\mathrm{M^{-1}\,s^{-1}}$
Reaction rate constant	k_{22}	7.1×10^6	$\mathrm{M^{-1}\,s^{-1}}$
First substrate concentration	s_{10}	5.0×10^{-3}	M

Table 2
Variable values of the biosensor parameters.

Parameters	Notation	Values interval	Dimension
Second substrate concentration	s_{20}	$[10^{-6}, 10^{-1}]$	M
First enzyme concentration	e_1	$[10^{-8}, 10^{-5}]$	M
Second enzyme concentration	e_2	$[10^{-8}, 10^{-5}]$	M
Enzyme layer thickness	d	$[5 \times 10^{-6}, 5 \times 10^{-4}]$	m
Diffusion layer thickness	δ	$[10^{-5}, 10^{-3}]$	m

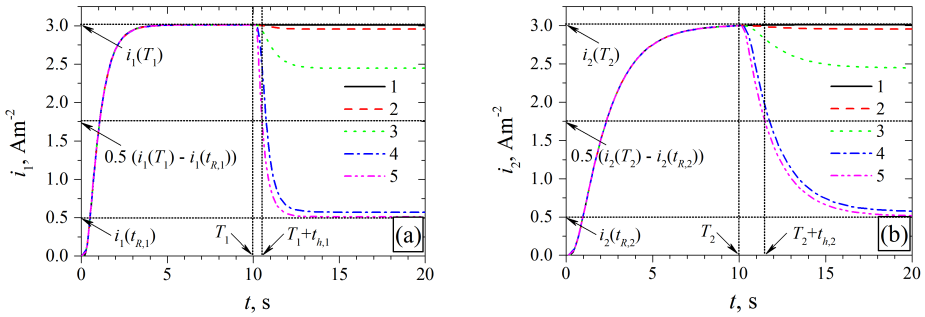

Fig. 1. The dynamics of the current for NCE (a) and CE (b) biosensors at the five concentrations s_{20} of the second substrate: 10^{-6} (1), 10^{-4} (2), 10^{-3} (3), 10^{-2} (4) and 10^{-1} (5) M.

3.3. *Biosensor Response*

The evolution of the biosensor response is displayed in Fig. 1 for NCE biosensor (Fig. 1a) and for CE biosensor (Fig. 1b). Calculations were carried out at the thickness $d = 3 \times 10^{-5}$ m of the enzymatic layer and the thickness $\delta = 10^{-5}$ m of the diffusion layer. The concentrations of catalase and peroxidase were $e_1 = 10^{-7}$ M and $e_2 = 10^{-6}$ M, respectively. Values of the second substrate concentration s_{20} varied from 10^{-6} to 10^{-1} M. The moments when the second substrate is poured into the solution were equal for both electrodes, $T_1 = T_2 = 10$ s. Values of the other parameters were as defined in Table 1.

As one can see from Fig. 1, the maximal current density is achieved at the end of the first phase of the biosensor operation when time $t = T_1$ for NCE biosensor (Fig. 1a) and $t = T_2$ for CE biosensor (Fig. 1b). The larger substrate concentration corresponds to a greater change in response, for both analysed biosensors (curves 4 and 5). Lower concentrations s_{20} of the second substrate have no significant impact in the response change (curves 1 and 2). The different boundary conditions mainly impact the half time of the steady-state. In order to achieve half of the steady-state current in both phases of the biosensor operation longer time was required for the Clark electrode based biosensor. The half time of the second phase steady-state for the largest concentration of the second substrate (curve 5, Figs. 1a and 1b) differs approximately two times: $t_{h,2} \approx 2 \times t_{h,1} = 1.4$ s.

Heterogenic constant k_s was calculated numerically to be $k_s = 1.74 \times 10^{-5}$ C^{-1} m^3, so that the values of both biosensor responses at the largest concentrations of the second substrate (curves 5, Figs. 1a and 1b) would be equal. The other steady-state currents were

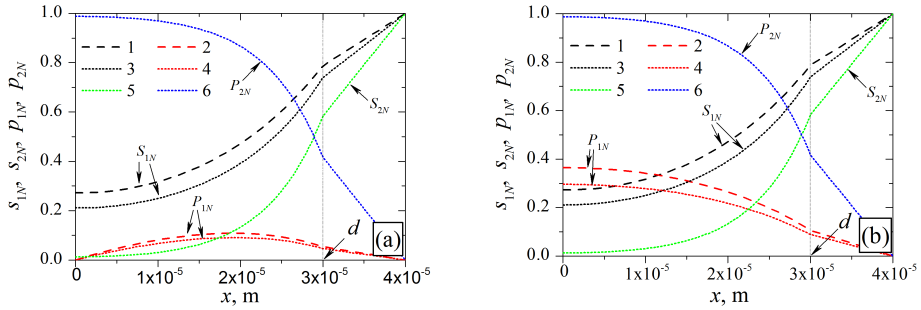

Fig. 2. Profiles of the normalized concentrations at time moments $t = T_1 = 5$ s (1, 2) and $t = 10$ s (3–6) for the NCE (a), and $t = T_2 = 20$ s (1, 2) and $t = 40$ s (3–6) for the CE biosensor (b). The second substrate was of the concentration $s_{20} = 10^{-3}$ M, the other parameters are the same as in Fig. 1.

calculated using the same value of heterogenic constant. The response values at the end of the operational phases are virtually identical for all the analysed concentrations s_{20} of the second substrate S_2. The responses at the steady-state for both models were compared digitally and the difference was non-existent.

4. Results and Discussion

Concentration profiles for both biosensors were compared at the different values of the concentration of the second substrate. The dependency of the half-time of the steady-state on the dimensionless reaction rate as well as on the Biot number was also calculated at different values of the second substrate concentration. The dependencies of the relative response and the relative sensitivity on the diffusion module were investigated at the different sets of parameter values.

4.1. *Concentration Profiles*

The normalization of concentrations is common when analysing biosensors behaviour (Morf *et al.*, 2011). The concentrations of both substrates and both products were normalized to the concentrations of the first and second substrates in the buffer solution,

$$s_{1n} = \frac{s_1}{s_{10}}, \qquad s_{2n} = \frac{s_2}{s_{20}}, \qquad p_{1n} = \frac{p_1}{s_{10}}, \qquad p_{2n} = \frac{p_2}{s_{10}}. \tag{28}$$

Figure 2 shows profiles of the normalized concentrations for both biosensors at the concentration $s_{20} = 10^{-3}$ M of the second substrate. The concentrations were captured at time moments $t = T_1 = 5$ s and $t = 10$ s for the NCE biosensor (Fig. 2a) and at $t = T_2 = 20$ s and $t = 40$ s for the biosensor based on the Clark electrode (Fig. 2b).

As it is seen from Fig. 2, the normalized concentrations of the molecular oxygen at both analysed time moments (curves 2 and 4) are relatively close for both biosensors in the entire space domain. A low concentration s_{2n} of the second substrate (curves 5, both pictures) explains the small difference between the concentrations p_{1n} of the first product. In

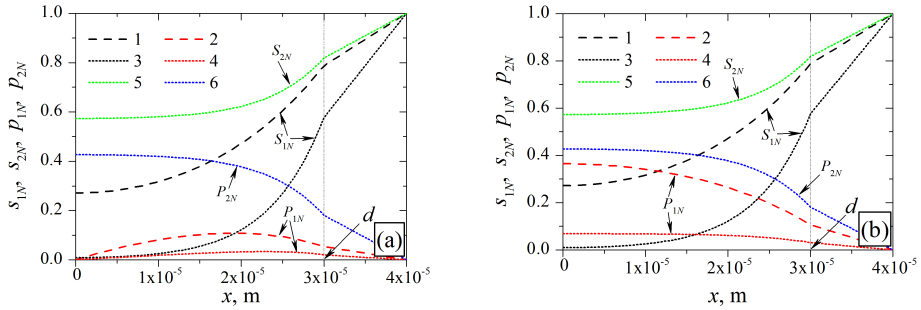

Fig. 3. The normalized concentrations of NCE (a) and CE (b) biosensors at the end of the first (1, 2) and second (3–6) operational stages at the concentration $s_{20} = 10^{-2}$ M. The other parameters are the same as in Fig. 2.

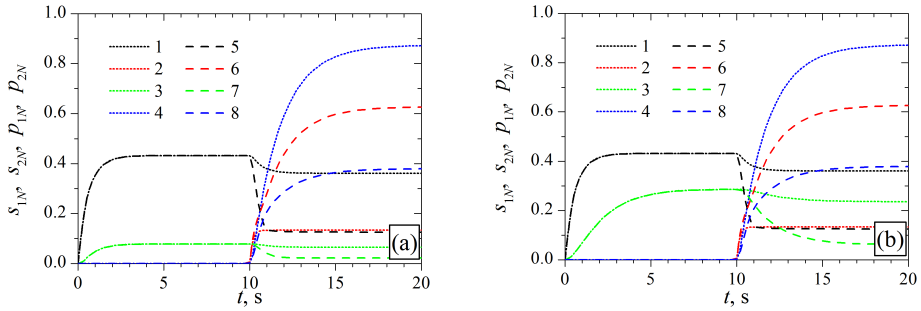

Fig. 4. The averaged concentrations of the first substrate (1, 5), the second substrate (2, 6), the first product (3, 7) and the second product (4, 8) for NCE (a) and CE (b) biosensors in the enzymatic layer. The concentration s_{20} of the second substrate were 10^{-3} M (1–4) and 10^{-2} M (5–8). The other parameters are the same as in Fig. 2.

case of CE biosensor (Fig. 2b) the oxygen (p_{1n}) is not consumed, therefore concentration of the first product is largest at the electrode surface (curves 2 and 4). The concentrations p_{2n} of the second product are practically identical for different electrodes used (curve 6).

The normalized concentrations of both substrates and both products at the concentration $s_{20} = 10^{-2}$ M of the second substrate are displayed in Fig. 3. Time moments for the NCE biosensor (Fig. 3a) and the Clark electrode (Fig. 3b) were the same as in Fig. 2.

As one can see from Fig. 3, an increase in the concentration of the second substrate (curves 5, parts (a) and (b)) results in a greater difference between the concentrations of the first reaction product at the end of operational phases (curves 2 and 4). The greater difference is observable for both analysed biosensors. The profiles of the concentrations of both substrates at both analysed operational stages are the same for both models (curves 1, 2 and 3, Figs. 3a and b). The dependence of the concentration averages for all the materials in the enzymatic layer on the time is depicted in Fig. 4. Two concentrations of the second substrate were analysed: $s_{20} = 10^{-3}$ and $s_{20} = 10^{-2}$ M, while the other parameter values were the same as in Fig. 2.

As it is seen from Fig. 4a, the half-time of the first steady-state is achieved at $t_{h,1} \approx 1$ s (curves 1, 3, 5 and 7) for the NCE biosensor. Larger concentration of the second substrate

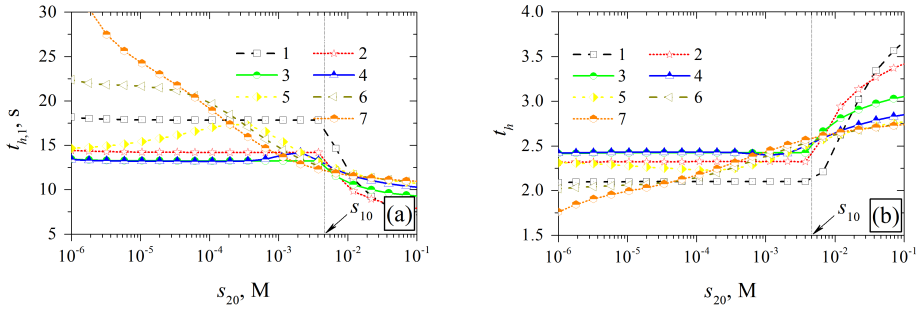

Fig. 5. The dependence of the NCE biosensor half-time (a) and the half-time ratio of both biosensors (b) on the second substrate concentration s_{20} at seven dimensionless reaction rates ξ: 10^{-3} (1), 10^{-2} (2), 10^{-1} (3), 100 (4), 10^{1} (5), 10^{2}(6) and 10^{3} (7), while the thicknesses of the enzymatic and diffusion layers were equal, $d = \delta = 10^{-4}$ M. The other parameters were the same as in Table 1.

(curve 6, compared to curve 2) corresponds to a decrease of the first substrate concentration (curves 1 and 5) as well as decrease of the first product concentration (curves 3 and 7). The concentration of the second product decreases approximately two times (curves 4 and 8). For CE biosensor (Fig. 4b) all the averaged concentrations are the same as for the CE biosensor (Fig. 4a), except for the concentration of the first product (curves 3 and 7). The half-time of the steady-state of the first product concentration is achieved only at $t_{h,2} \approx 1$ s. The absolute values of the first product concentration for the CE electrode are noticeably larger than the ones for the NCE electrode. This leads to a larger decrease of the first product concentration averages in time, for the larger concentration of the second substrate (curve 7). However, the relative difference between concentrations of the first product for both biosensors is the same (curves 3 and 7, both parts of the Fig. 4).

4.2. *Response Time*

The impact of the second substrate concentration on the half-time of the steady-state was analysed at seven different dimensionless reaction rates ξ, varying from 10^{-3} to 10^{3}. The thicknesses of enzymatic and diffusion layers were considered to be equal at $d = \delta = 10^{-4}$ m. The concentration of the second substrate was changed as in Table 2. The other parameter values were constant as in Table 1. The dependence of the half-time for the NCE biosensor is displayed in Fig. 5a. To investigate the difference between the electrodes, the following dimensionless ratio t_h of the half-times to the steady-state for both biosensors was introduced and called the half-time ratio:

$$t_h = \frac{t_{h,2}}{t_{h,1}}. \tag{29}$$

As one can see from Fig. 5a, the half-time of the steady-state is a complex function of the second substrate concentration s_{20} and the dimensionless reaction rate ξ. For relatively small dimensionless reaction rates ($\xi < 1$, curves 1–3) the influence of the first substrate concentration ($s_{10} = 5 \times 10^{-3}$ M) is especially noticeable. When

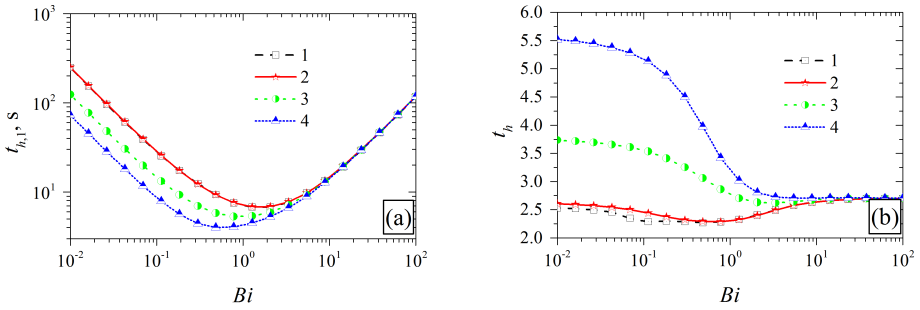

Fig. 6. The dependence of the half-time for the NCE biosensor (a) and of the half-time ratio (b) on the Biot number Bi at four different concentrations s_{20} of the second substrate: 10^{-6} (1), 10^{-3} (2), 10^{-2} (3) and 10^{-1} (4) M. The thicknesses of the enzymatic and diffusion layers were changed according to Table 2. The other parameters were as in Table 1.

$s_{20} < s_{10}$ and $\xi < 1$, the half-time is practically a stagnant function of s_{20}. For relatively large concentrations of the second substrate ($s_{20} > s_{10}$) and $\xi < 1$, the half-time of the steady-state is a decreasing function of the concentration s_{20} of the second substrate. The decrease is mostly drastic for the smallest dimensionless reaction rate ($\xi = 10^{-3}$, curve 1). The influence of the second substrate concentration s_{20} at relatively small dimensionless reaction rates is clearly noticeable in Fig. 5b, curves 1–4. For the intermediate dimensionless reaction rate of $\xi = 10$ (curve 1, Fig. 5a) a noticeable shoulder on the curve appears at approximately $s_{20} = 2 \times 10^{-4}$ M, as well as a smaller shoulder of curve 5, at $s_{20} = 2 \times 10^{-4}$ M. Similar non-monotonicity of the half-time function was noticed in the kinetics of other biosensors as well (Bartlett *et al.*, 1997; Baronas *et al.*, 2003).

The influence of the Biot number on the half-time of the steady-state was analysed by changing the values of the enzymatic and diffusion layer thicknesses according to Table 2. Concentrations of catalase and peroxidase were considered to be equal at $e_1 = e_2 = 10^{-6}$ M, while the other parameters were kept constant as listed in Table 1. The values of the second substrate concentration s_{20} were changed between 10^{-6} and 10^{-1} M. The calculation results for NCE biosensor are displayed in Fig. 6.

As it is seen from Fig. 6a, the greatest half-times to the steady-state are at the relatively small and relatively large Biot numbers Bi. An increase at both ends of the interval of the analysed values of Bi can be explained by changing thicknesses, the enzymatic and the diffusion, therefore at both ends the diffusion regime predetermines the biosensors behaviour. For the relatively small values of Biot number ($Bi < 1$) the impact of the second substrate concentration on the half-time is noticeable: smaller values of substrate concentration represent larger values of the half-time. No influence of the second substrate concentration is visible for the relatively large values of Biot number ($Bi > 1$). As one may see from Fig. 6b, the influence of the analysed boundary condition is stronger at smaller values of the Biot number, especially for the largest analysed concentration of the second substrate ($s_{20} = 0.1$, curve 4). The ratio (29) of the half-times for both biosensors is non-monotonous function of Bi for the smaller concentrations of the second substrate (curves 1 and 2, Fig. 6b).

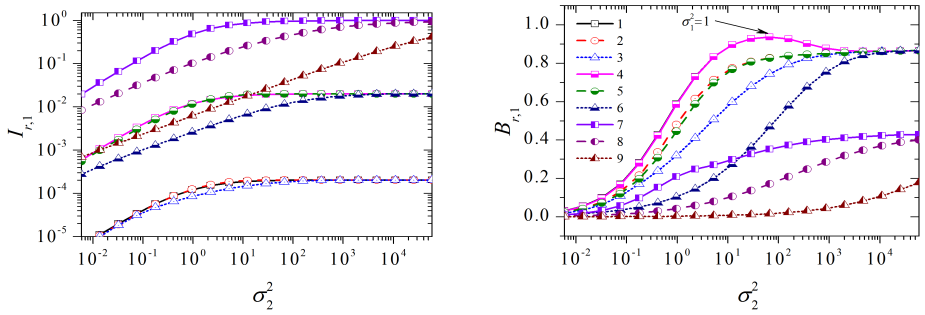

Fig. 7. The dependence of the relative response (a) and relative sensitivity (b) on the second diffusion module σ_2^2 at three different concentrations s_{20} of the second substrate: 10^{-6} (1–3), 10^{-4} (4–6), 10^{-2} (7–9) M. The concentration e_1 of the first enzyme was 10^{-8} (1, 4, 7), 5×10^{-7} and 10^{-6} M. The other parameters were as in Table 1.

4.3. *The Impact of the Diffusion Module*

The influence of the second diffusion module on the relative response (Fig. 7a) and relative sensitivity (Fig. 7b) was investigated at three very different concentrations s_{20} of the second substrate (10^{-6}, 10^{-4} and 10^{-2} M) and three different concentrations e_1 of the first enzyme (10^{-8}, 5×10^{-7} and 10^{-6} M) for NCE biosensor. By changing the thickness of the enzymatic layer and the concentration of the second substrate, as defined in Table 2, the values σ_2^2 of the second diffusion module changes in 7 orders of magnitude. The dependencies at the same values of the parameters for the Clark-type biosensor were exactly identical to the ones displayed in Fig. 7, therefore they are not depicted separately.

As one can see from Fig. 7a, the relative response is a monotonous increasing function of the second diffusion module for all the analysed values of the biosensor parameters. The smallest concentrations ($s_{20} = 10^{-6}$ M) of the second substrate (curves 1–3) correspond to the lowest relative responses of the biosensor without any considerable effect of the first enzyme concentration. For the largest analysed concentrations ($s_{20} = 10^{-2}$ M) of the second substrate (curves 7–9) the relative responses are considerably larger, with a noticeable impact of the first enzyme concentration. The lowest analysed concentration $e_1 = 10^{-8}$ M of the first enzyme (curve 7) corresponds to the largest possible response ($I_{r,1} \approx 1$), when $\sigma_2^2 > 10$. The increase of the first enzyme concentration leads to the lower values of the relative response (curves 7–9 corresponding to $e_1 = 10^{-8}, 5 \times 10^{-7}, 10^{-5}$ M). The biggest relative difference between the responses for $s_{20} = 10^{-2}$ is approximately 100, reached at $\sigma_2^2 = 1$ for the largest and smallest concentrations of the first enzyme (curves 7 and 9).

However, for the largest relative responses the sensitivities are the lowest (curves 7–9, Fig. 7b), with a small increase for the larger values of the diffusion module. The sensitivity $B_{r,1}$ is more than 0.4 when $s_{20} \leqslant 10^{-4}$ M and $\sigma_2^2 > 1$ (curves 1–5). For the smallest concentrations of the first enzyme ($e_1 = 10^{-8}$ M) and smallest concentrations of the second substrate ($s_{20} \leqslant 10^{-4}$ M) largest overall sensitivity is achieved (curves 1 and 4). A non-monotonicity is noticeable at $\sigma_2^2 \approx 100$ for the mentioned curves, as the point of extrema corresponds to the unity of the first diffusion module.

5. Conclusions

Two computational models presented in this paper can be successfully used to investigate the behaviour of the biosensors utilizing different boundary conditions. Digitally, neither of the distinct models has a significant advantage over the other, as the simulation times of both computational models does not differ more than twice for any of the analysed parameter values.

By changing the parameter values the output of both computational models can be manipulated in the variety of ways. The half-time of the steady-state, the response and the sensitivity of both models at the same parameter values were compared. At the concrete parameter values the impact of the different electrodes reaches as much as 3.5 (Fig. 5b) and 5.5 (Fig. 6a) times in the relative difference for the half-times of the steady-state response. No differences were noted while comparing the responses and sensitivities at the transient or steady-state state conditions.

Relative response of the biosensor is a monotonous increasing function of the second diffusion module σ_2^2. The largest relative responses are achieved at the smallest concentrations of the first enzyme and the largest concentrations of the second substrate (Fig. 7a). However, with a before-mentioned parameter values the relative sensitivity of the biosensor is the lowest. The non-monotonicity in the dependence of the relative sensitivity on the second diffusion module was noted, as a largest possible sensitivity of $B_{r,1} \approx 1$ is achieved at $\sigma_2^2 \approx 100$ and $\sigma_1^2 \approx 1$ (Fig. 7b).

Acknowledgement. This research is funded by the European Social Fund under the Global Grant measure, project No. VP1-3.1-ŠMM-07-K-01-073/MTDS-110000-583.

References

Ahuja, P. (2010). *Introduction to Numerical Methods in Chemical Engineering*. Texas Tech University Press, Lubbock.

Akkaya, A., Pazarlioglu, N.K., Dinckaya, E. (2009). Determination of 5-aminosalicylic acid by catalase-peroxidase based biosensor. *Electroanalysis*, 21(16), 1805–1810.

Andersen, M.B., Hsuanyu, Y., Welinder, K.G., Schneider, P., Dunford, H.B. (1991). Spectral and kinetic-properties of oxidized intermediates of coprinus-cinereus peroxidase. *Acta Chemica Scandinavica*, 45(10), 1080–1086.

Aris, R. (1975). *The Mathematical Theory of Diffusion and Reaction in Permeable Catalysts. The Theory of the Steady State*. Clarendon, Oxford.

Ašeris, V., Baronas, R., Kulys, J. (2012). Modelling the biosensor utilizing parallel substrates conversion. *Journal of Electroanalytical Chemistry*, 685, 63–71.

Baronas, R., Kulys, J. (2008). Modelling amperometric biosensors based on chemically modified electrodes. *Sensors*, 8(8), 4800–4820.

Baronas, R., Ivanauskas, F., Sapagavas, M. (2002). Reliability of one dimensional model of moisture diffusion in wood. *Informatica*, 13(4), 405–416.

Baronas, R., Ivanauskas, F., Kulys, J. (2003). The influence of enzyme membrane thickness on the response of amperometric biosensors. *Sensors*, 3(7), 248–262.

Baronas, R., Ivanauskas, F., Kulys, J. (2010). *Mathematical Modeling of Biosensors*. Springer, Dordrecht.

Bartlett, P.N., Birkin, P.R., Wallace, E.N.K. (1997). Oxidation of β-nicotinamide adenine dinucleotide (NADH) at poly(aniline)-coated electrodes. *Journal of the Chemical Society, Faraday Transactions*, 93(10), 1951–1960.

Bartlett, P.N., Toh, C.S., Calvo, E.J., Flexer, V. (2008). Modelling biosensor responses. In: Bartlett, P.N. (Ed.), *Bioelectrochemistry: Fundamentals, Experimental Techniques and Applications*. Wiley, Chichester.

Basov, I., Švitra, D.(2000). A possibility of taking into consideration of insulin "age structure" for modeling blood glucose dynamics. *Informatica*, 11(1), 87–96.

Bieniasz, L.K. (1993). Use of dynamically adaptive grid techniques for the solution of electrochemical kinetic equations. Part 1. Introductory exploration of the finite difference adaptive moving grid solution of the one-dimensional, fast homogeneous reaction-diffusion problem with a reaction layer. *Journal of Electroanalytical Chemistry*, 360(1-2), 119–138.

Bieniasz, L.K. (2004). Use of dynamically adaptive grid techniques for the solution of electrochemical kinetic equations. Part 15: Patch-adaptive simulation of example transient experiments described by Nernst–Planck-electroneutrality equations in one-dimensional space geometry. *Journal of Electroanalytical Chemistry*, 565(2), 273–285.

Bieniasz, L.K., Britz, D. (2004). Recent developments in digital simulation of electroanalytical experiments. *Polish Journal of Chemistry*, 78, 1195–1219.

Bisswanger, H. (2008). *Enzyme Kinetics: Principles and Methods*, 2nd ed. Wiley-VCH, Weinheim.

Britz, D. (2005). *Digital Simulation in Electrochemistry*, 3rd ed. Springer, Berlin.

Britz, D., Baronas, R., Gaidamauskaitė, E., Ivanauskas, F. (2009). Futher comparisons of finite diference schemes for computational modelling of biosensors. *Nonlinear Analysis: Modelling and Control*, 14(4), 419–433.

Cooper, J.M., Cass, A.E.G. (2003). *Biosensors – A Practical Approach*, 2nd ed. Oxford University Press, Oxford.

Crank, J., Nicolson, P. (1947). A practical method for numerical evaluation of solutions of partial differential equations of the heat conduction type. *Proceedings of the Cambridge Philosophical Society*, 43, 50–64.

Dabulytė-Bagdonavičienė, J., Ivanauskas, F., Razumas, V. (2011). The computational modelling of the kinetics of ascorbic acid palmitate hydrolysis by lipase considering diffusion. *Central European Journal of Chemistry*, 9(4), 712–719.

Kleiza, J., Sapagovas M., Kleiza V. (2007). The extension of the van der Pauw method to anisotropic media. *Informatica*, 18(2), 253–266.

Kulys, J., Sorochinski, V.V., Vidziunaite, R. (1986). Transient response of bienzyme electrodes. *Biosensors*, 2(3), 135–146.

Kulys, J., Krikstopaitis, K., Ziemys, A. (2000). Kinetics and thermodynamics of peroxidase- and laccase-catalyzed oxidation of *N*-substituted phenothiazines and phenoxazines. *Journal of Biological Inorganic Chemistry*, 5(3), 333–340.

Mell, L.D., Maloy, J.T. (1975). A model for the amperometric enzyme electrode obtained through digital simulation and applied to the immobilized glucose oxidase system. *Analytical Chemistry*, 47(2), 299–307.

Morf, W.E., Wal, P.D.v.d., Pretsch, E., Rooij, N.F.d. (2011). Theoretical treatment and numerical simulation of potentiometric and amperometric enzyme electrodes and of enzyme reactors. *Journal of Electroanalytical Chemistry*, 657(1), 1–12.

Press, W.H., Teukolsky, S.A., Vetterling, W.T., Flannery B.P. (2007). *Numerical Recipes: The Art of Scientific Computing*, 3rd ed. Cambridge University Press, New York.

Rickus, J.L. (2005). Impact of coenzyme regeneration on the performance of an enzyme based optical biosensor: a computational study. *Biosensors and Bioelectronics*, 21(6), 965–972.

Rodriguez-Lopez, J., Ros-Martinez, J., Varon, R., Garcia-Canovas, F. (1992). Calibration of a Clark-type oxygen electrode by tyrosinase-catalyzed oxidation of 4-tert-butylcatechol. *Analytical Biochemistry*, 202(2), 356–360.

Sadana, A., Sadana, N. (2010). *Handbook of Biosensors and Biosensor Kinetics*. Elsevier, Amsterdam.

Samarskii, A.A. (2001). *The Theory of Difference Schemes*. Dekker, New York.

Scheller, F.W., Schubert, F., Fedrowitz, J. (1997). *Frontiers in Biosensorics*. Birkhäuser, Basel.

Schulmeister, T. (1990). Mathematical modelling of the dynamic behaviour of amperometric enzyme electrodes. *Selective Electrode Reviews*, 12(2), 203–260.

Žilinskas, A., Baronas, D. (2011). Optimization-based evaluation of concentrations in modeling the biosensor-aided measurement. *Informatica*, 22(4), 589–600.

V. Ašeris is a PhD student at the Faculty of Mathematics and Informatics of Vilnius University. He obtained BSc degree in 2007 and MSc degree in 2009, both in the field of Software Engineering in Vilnius University. His research interests are computational modelling of biosensors.

R. Baronas is a professor and serves as chair of the Department of Software Engineering at Vilnius University. Prof. Baronas received his MSc degree in Applied Mathematics in 1982. He obtained his PhD degree in Computer Science in 2000 from the Vilnius University. His teaching and research interests lie in the areas of database systems and computational modelling of biochemical processes.

J. Kulys is a professor of physical chemistry. As of 1974 he works as the head of department of Enzyme Chemistry of the Institute of Biochemistry of Vilnius University. As of 2001 he also works as the head of the department of Chemistry and Bioengineering of Vilnius Gediminas Technical University. He was awarded by the State Science Prize (1987), the Baltic Assembly Premium of Science (1995), National Science Premium (2002), was elected as Academician of the Lithuania Academy of Sciences (1996). He is an editor of the journal "Biosensors & Bioelectronics", member of the editorial board of journals "The Open Nanoscience Journal", "The Open Enzyme Inhibition Journal", "The Open Biotechnology Journal", "Biologija", "Nonlinear Analysis: Modelling and Control". The main scientific interests cover chemical problems of biocatalysis and biosensors.

Skaitinis dvifermenčio jutiklio modeliavimas su skirtingomis pradinėmis ir kraštinėmis sąlygomis

Vytautas AŠERIS, Romas BARONAS, Juozas KULYS

Darbe skaitmeniškai nagrinėjami du skirtingi matematiniai amperometrinių dvifermenčių biojutiklių veikimo modeliai. Modeliai skiriasi kraštine sąlyga, aprašančia elektrodo veikimą. Išnagrinėta pradinių ir kraštinių sąlygų įtaka biojutiklio veikimui įvairioms parametrų reikšmėms.

Skaitinis modeliavimas atliktas stacionariojoje ir tarpinėje būsenose naudojant baigtinių skirtumų metodą. Palyginus modeliavimo rezultatus nustatyta, kad kai kurie apskaičiuojami parametrai (pvz. atsakas ir jautris) yra vienodi abiems modeliams, o kiti (pvz. stacionariosios būsenos puslaikis) skiriasi.